

Numerical analysis of the spin-dependent dark current in microcrystalline silicon solar cells

T. Brammer^{a)} and H. Stiebig

Institute of Photovoltaics, Forschungszentrum Jülich, 52425 Jülich, Germany

K. Lips^{b)}

Abt. Silizium-Photovoltaik, Hahn-Meitner Institut, Kekuléstr. 5, 12489 Berlin, Germany

(Received 22 March 2004; accepted 29 June 2004)

We present a detailed analysis of the voltage dependence of dangling bond recombination in microcrystalline silicon *p-i-n* diodes observed in the forward dark current at room temperature by electrically detected magnetic resonance (EDMR). The EDMR response is numerically simulated with physically reasonable parameters that are well suited to fully describe the electronic behavior of the diodes. A sign reversal as observed for amorphous silicon diodes is predicted at high voltages. The basic mechanism causing the sign reversal is shown to be due to space charge. The high sensitivity of the EDMR response to various material parameters is demonstrated. © 2004 American Institute of Physics. [DOI: 10.1063/1.1787163]

A unique experimental method that allows direct access to recombination in amorphous silicon (*a-Si:H*),^{1,2} crystalline silicon,^{3–10} and microcrystalline silicon ($\mu\text{c-Si:H}$)¹¹ devices is electrically detected magnetic resonance (EDMR). The key advantage of EDMR is its high sensitivity and selectivity for certain paramagnetic states. This is due to the fact that the paramagnetic states are identified through small conductivity changes induced by electron spin resonance (ESR). Thus, the influence of a specific recombination channel on device performance can be studied. For the interpretation of the EDMR results, numerical device models are indispensable to account for the complex interplay between recombination and transport, especially when space-charge effects due to localized states become important. This is the case in $\mu\text{c-Si:H}$. The key advantage of EDMR modeling is the fact that the influence of a single material parameter, the capture cross section, can be simulated and experimentally verified. Hence, comparison to EDMR results could help to determine unknown material parameters of $\mu\text{c-Si:H}$.

Previous EDMR studies have shown that the interaction of the microwave with neutral dangling bonds (Landé factor $g=2.005$) changes the dark forward current of $\mu\text{c-Si:H}$ *p-i-n* diodes.¹¹ This is related to the fact that the capture probability of electrons into neutral defects depends on the relative orientation of their spins, e.g., in triplet configuration, the trapping time is by two orders of magnitude longer than in singlet configuration.¹² At ESR resonance, the average capture time is reduced. This changes the recombination rate and, hence, the device current. One of the surprising results of the previous EDMR study¹¹ was that unlike in *a-Si:H* diodes, in $\mu\text{c-Si:H}$ diodes only a positive current change (enhancing) could be detected. The typical sign reversal (quenching) of the EDMR signal above the turn-over voltage V_C , which is so prominent for *a-Si:H* and was related to electric field reversal in the *i* layer,¹¹ is absent in $\mu\text{c-Si:H}$. This led to the conclusion that *p-i-n* diodes based on $\mu\text{c-Si:H}$ are governed by a different balance of drift and diffusion than *a-Si:H* diodes. In this work, this discrepancy

is analyzed by means of numerical device simulations. In addition, we will show that the EDMR behavior is very sensitive to the defect density (N_d), electron and hole mobility ($\mu_e/\mu_h=3$), band tail slope, and the external series resistance (R_S). Details of the experiment and the simulation software which numerically solves the semiconductor equations can be found in Refs. 11 and 13, respectively.

The EDMR response of the dark current is defined as $\Delta J/J=(J^*-J)/J$ where J^* and J are the dark currents with and without applied microwave, respectively. For the simulation of J^* , the capture cross section for electrons into neutral states (defects occupied by a single electron) is increased by a small fraction $\Delta\sigma/\sigma=0.25\%$. The magnitude of $\Delta\sigma/\sigma$ is determined by the ratio of the singlet and triplet capture rate coefficients. The capture cross section of positively charged defects (unoccupied defect) and negatively charged defects (two electrons occupy the defect state) as well as all other parameters are kept constant, because they are not spin dependent. Figure 1 depicts the measured (●) and simulated (lines) EDMR signal of the $\mu\text{c-Si:H}$ diode deposited by plasma-enhanced chemical vapor deposition at around 200 °C.¹⁴ The simulations are carried out with and without

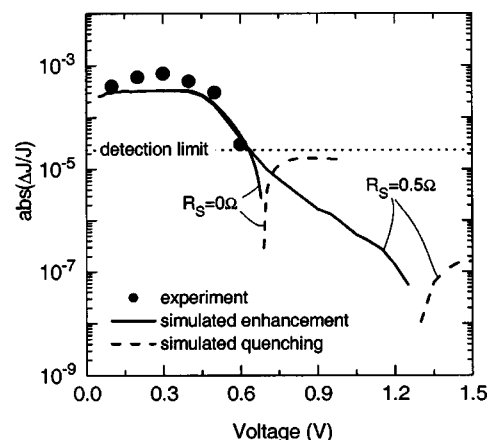


FIG. 1. Measured (●) and simulated (lines) EDMR signal of a $\mu\text{c-Si:H}$ *p-i-n* diode. The solid symbol and line type denote enhanced current at EDMR ($\Delta J > 0$) and the dashed line denotes quenching ($\Delta J < 0$).

^{a)}Electronic mail: t.brammer@fz-juelich.de

^{b)}Electronic mail: lips@hmi.de

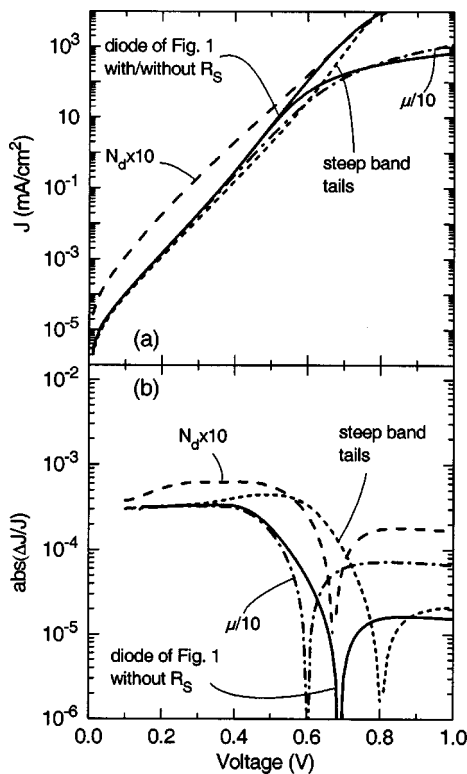


FIG. 2. (a) Simulated dark J - V curves and (b) simulated EDMR signals of four $\mu\text{c-Si:H}$ p - i - n diodes with different i -layer properties: A larger defect density (---), a smaller mobility (- · - ·), and steeper band tails (· · · ·) in comparison to the diode of Fig. 1 (—). For all simulations in (b) $R_S = 0 \Omega$.

R_S which is usually between 0.5 and 1.5 Ω for diodes with an area of $1 \times 1 \text{ cm}^2$. The measurement on $\mu\text{c-Si:H}$ diodes only gives positive current changes (enhancing) in contrast to the signal of $a\text{-Si:H}$ diodes where negative values (quenching) are found above a voltage of 0.7 V.¹¹ For small bias, the simulated EDMR signal matches well with the measured signal solely by considering the minor change of the capture cross section $\Delta\sigma$. The enhancement (solid line) is due to the increase in the recombination rate. For $R_S = 0 \Omega$, the simulations predict a sign reversal (dashed line) of the EDMR signal at $V_C \approx 0.7 \text{ V}$ so that the signal is, in principle, comparable to the signal found for diodes based on $a\text{-Si:H}$.¹¹ The calculated signal intensity for $V > V_C$ is, however, below the present detection limit which is represented by the dotted line in Fig. 1. For $R_S = 0.5 \Omega$, the sign reversal occurs only for $V > 1.3 \text{ V}$. Additionally, the signal intensity is reduced. Hence, for the detection of the sign reversal of $\mu\text{c-Si:H}$ diodes, it is essential to lower the detection limit of the EDMR setup and to ensure that R_S is well below 0.5 Ω .

Next, the influence of the material properties of the i layer on the EDMR signal and the dark current density versus voltage (J - V) curves is illustrated in more detail (Fig. 2). The variation of the parameters is performed with respect to the simulated diode shown in Fig. 1 which was derived using $N_d = 10^{15} \text{ cm}^{-3}$, $\mu_e = 10 \text{ cm}^2/\text{V s}$ and an inverse logarithmic valence-band tail slope of $E_0 = 25.9 \text{ meV}$ (the inverse logarithmic conduction-band tail slope is assumed to be $E_0/2$). These values lead to a good fit with the experimental dark J - V curves.¹³ The effect of R_S , the decrease in J for $J > 1 \text{ mA/cm}^2$, is exemplarily demonstrated for this diode [bold lines in Fig. 2(a)]. For the other simulated diodes, only one of the three mentioned parameters is changed and $R_S = 0 \Omega$.

Increasing N_d (---) by a factor of 10 leads to an increase of the dark current and the EDMR signal. This is caused by the higher recombination rate. V_C is hardly affected. Reducing μ_e by a factor of 10 (- · - ·) has no effect on the dark current and the EDMR signal for $V < 0.45 \text{ V}$. For larger voltages, the dark current decreases. The EDMR signal increases above V_C which is about 0.1 V smaller. In the case of very steep band tails ($E_0 \rightarrow 0 \text{ eV}$), the dark current and the EDMR signal below 0.3 V do not change. For $V > 0.3 \text{ V}$, the dark current decreases and V_C is increased by about 0.1 V. These simulations demonstrate that EDMR modeling can be used to narrow the material parameter space for $\mu\text{c-Si:H}$.

Common to all simulated diodes in Fig. 2 is the fact that well below V_C the dark current increases exponentially with V . This is the typical ideal diode J - V curve if space charge due to trapped charge carriers is negligible. Above V_C , the dark current increases subexponentially with V . The reason for this behavior is that for $V > V_C$, space charge hinders the transport of charge carriers. This is particularly apparent for the diode with the reduced mobility which promotes capture of charge carriers into localized states (band tails and defects). When the capture cross section for neutral defects increases due to the ESR microwave, the space charge is increased and the current is further reduced. This reduction leads to the negative ΔJ . The influence of the space charge becomes most prominent when the electric field in the i layer has reversed.

In summary, the EDMR signal of $\mu\text{c-Si:H}$ diodes was investigated by means of numerical simulations. A good agreement between measured and simulated data is found for the positive EDMR effect at low voltage which is caused by the increased recombination rate in the i layer. The simulations predict a sign reversal of the EDMR signal for $\mu\text{c-Si:H}$ diodes as observed for $a\text{-Si:H}$ diodes, which rules out the previously postulated general difference between both kinds of diodes. The sign reversal of the EDMR effect is shown to be due to space-charge effects. The anticipated signal intensity for $\mu\text{c-Si:H}$ diodes is, however, below the present detection limit. Additionally, series resistance can strongly affect the EDMR signal intensity. A high sensitivity of EDMR to various material parameters is predicted.

¹K. Lips and W. Fuhs, *J. Appl. Phys.* **74**, 3993 (1993).

²G. Kawachi, C. F. O. Graeff, M. S. Brandt, and M. Stutzmann, *Phys. Rev. B* **54**, 7957 (1996).

³I. Solomon, *Solid State Commun.* **20**, 215 (1976).

⁴J. T. Krick, P. M. Lenahan, and G. J. Dunn, *Appl. Phys. Lett.* **59**, 3437 (1991).

⁵F. C. Rong, G. J. Gerardi, W. R. Buchwald, E. H. Poindexter, M. T. Umlor, D. J. Keeble, and W. L. Warren, *Appl. Phys. Lett.* **60**, 610 (1992).

⁶C. H. Seager, E. L. Venturini, and W. K. Schubert, *Appl. Phys. Lett.* **60**, 1732 (1992).

⁷J. H. Stathis and D. J. DiMaria, *Appl. Phys. Lett.* **61**, 2887 (1992).

⁸P. Christmann, C. Wetzel, B. K. Meyer, A. Asenov, and A. Endros, *Appl. Phys. Lett.* **60**, 1857 (1992).

⁹Y. Kamigaki, T. Miyazaki, N. Yoshihiro, K. Watanabe, and K. Yokogawa, *J. Appl. Phys.* **84**, 2193 (1998).

¹⁰T. D. Mishima, P. M. Lenahan, and W. Weber, *Appl. Phys. Lett.* **76**, 3771 (2000).

¹¹K. Lips, C. Boehme, and W. Fuhs, *IEE Proc.-G: Circuits, Devices Syst.* **150**, 309 (2003).

¹²C. Boehme and K. Lips, *Phys. Status Solidi B* **1**, 1255 (2004).

¹³T. Brammer and H. Stiebig, *J. Appl. Phys.* **94**, 1035 (2003).

¹⁴O. Vetterl, F. Finger, R. Carius, P. Hapke, L. Houben, O. Kluth, A. Lambert, A. Mück, B. Rech, and H. Wagner, *Sol. Energy Mater. Sol. Cells* **62**, 97 (2000).